molecules

MDPI

Article

Renieramycin T Inhibits Melanoma B16F10 Cell Metastasis and Invasion via Regulating Nrf2 and STAT3 Signaling Pathways

Baohua Yu [1,†], Jing Liang [1,†], Xiufang Li [2,†], Li Liu [1], Jing Yao [3], Xiaochuan Chen [4,*] and Ruijiao Chen [1,3,*]

[1] Department of Pediatric Surgery, Affiliated Hospital of Jining Medical University, Jining 272067, China
[2] College of Pharmacy, Heze University, Heze 274015, China
[3] College of Basic Medicine, Jining Medical University, Jining 272067, China
[4] Key Laboratory of Green Chemistry and Technology of Ministry of Education, College of Chemistry, Sichuan University, Chengdu 610064, China
* Correspondence: chenxc@scu.edu.cn (X.C.); chenrj@mail.jnmc.edu.cn (R.C.); Tel.: +86-28-8541-2095 (X.C.); +86-53-7361-6216 (R.C.)
† These authors contributed equally to this work.

Abstract: As one of marine tetrahydroisoquinoline alkaloids, renieramycin T plays a significant role in inhibiting tumor metastasis and invasion. However, the effect of renieramycin T on inflammation-related tumor metastasis and invasion is still unknown, and its mechanisms remain unclear. Here we established an inflammation-related tumor model by using the supernatant of RAW264.7 cells to simulate B16F10 mouse melanoma cells. The results indicate that renieramycin T suppressed RAW264.7 cell supernatant-reduced B16F10 cell adhesion to a fibronectin-coated substrate, migration, and invasion through the matrigel in a concentration-dependent manner. Moreover, Western blot results reveal that renieramycin T attenuated the phosphorylation of STAT3 and down-regulated the expression of Nrf2. Together, the above findings suggest a model of renieramycin T in suppressing B16F10 cancer cell migration and invasion. It may serve as a promising drug for the treatment of cancer metastasis.

Keywords: renieramycin T; tumor metastasis and invasion; p-STAT3; Nrf2

Citation: Yu, B.; Liang, J.; Li, X.; Liu, L.; Yao, J.; Chen, X.; Chen, R. Renieramycin T Inhibits Melanoma B16F10 Cell Metastasis and Invasion via Regulating Nrf2 and STAT3 Signaling Pathways. *Molecules* **2022**, *27*, 5337. https://doi.org/10.3390/molecules27165337

Academic Editor: Claudiu T. Supuran

Received: 18 June 2022
Accepted: 18 August 2022
Published: 22 August 2022

1. Introduction

A malignant tumor has a higher metastatic capacity; the way of metastasizing includes tissue, blood and lymph, etc. [1]. Melanoma is a highly malignant skin tumor, which has various characteristics, such as high morbidity and mortality rate and early transfer [2–6]. Research shows that the most people die from metastatic carcinoma rather than primary carcinoma [1]. Therefore, restraining tumor migration and invasion may provide a valid strategy for tumor treatment.

The tumor microenvironment comprises a variety of nonmalignant stromal cells that play a pivotal role in tumor progression and metastasis [7]. Among them, tumor-associated macrophages (TAMs) are one of the most notable migratory hematopoietic cell types [8]. Clinical studies show that an increased number of TAMs frequently correlates with angiogenesis, metastasis, and poor prognosis [9]. Nevertheless, there is a consensus view that macrophage polarization is strongly related to tumor stage, suggesting that a dynamic switching from M1 phenotype, during the early phases of chronic inflammation, to an M2-like one might occur in established tumors. RAW264.7, a precursor of macrophage cell lines, was widely used in M1/M2 macrophage function research [10]. Moreover, RAW264.7 supernatant was proven to contain many inflammatory cytokines and chemokines, which were applied to establish an inflammation-related micro-environment [11].

As a transcription factor, NF-E2-relatedfactor 2 (Nrf2) mediate tumor progression via accelerated tumor proliferation [12–14]. It is verified that Nrf2 is up-regulated in lung, head, and neck squamous cell carcinoma tissues [15]. Further investigation shows that

overexpression of Nrf2 enhances tumor chemo-resistance in some lung carcinoma, breast adenocarcinoma, and neuroblastoma cell lines [16]. It is reported that loss of Nrf2 in an oncogenic context-dependent manner can enhance cellular plasticity and motility, in part by using TGF-β/Smad signaling [17], and Nrf2 activation promotes lung cancer metastasis by inhibiting the degradation of Bach1 [18]. Nrf2 accumulation in lung cancers causes the stabilization of Bach1 by inducing HO-1, the enzyme catabolizing heme.

It is reported that aberrant STAT3 activation in tumor cells is associated with cell proliferation, cell survival, invasion, angiogenesis, and metastasis [19–23]. Conversely, targeting STAT3 activation inhibits tumor growth and metastasis both in vitro and in vivo without affecting normal cells, thus suggesting that STAT3 could be a valid molecular target for cancer therapy [24]. Moreover, STAT3 participates in tumor migration and invasion [25–28], and persistent activation of STAT3 in epithelial/tumor cells is linked to multiple human malignancies, including inflammation-associated cancer [29].

Marine tetrahydroisoquinoline alkaloids, are one kind of natural product that have a wide range of bioactivities, including anti-tumor, anti-bacteria, anti-virus, anti-inflammation activities, etc. [30]. Ecteinascidin-743 (ET-743) is the first marine antitumor drug to treat soft tissue sarcoma (STS) approved by the European Union in October 2007 [31]. Renieramycin T (RT), a bistetrahydroisoquinolinequinone that is extracted from the Thai blue sponge *Xestospongia* sp., for this study, was self-synthesized by Dr. Xiaochuan Chen from Sichuan University [32]. RT and its derivatives exhibited potent cytotoxicity against human lung cancer cells [33–36]. Nevertheless, the function of RT in mediating inflammation-related migration and invasion remains unclear.

In this study, we established an inflammation-related tumor model by using the supernatant of RAW264.7 cells to simulate B16F10 mouse melanoma cells. Moreover, we showed that RT suppressed RAW264.7 cell supernatant-reduced B16F10 cell adhesion to fibronectin-coated substrate, migration, and invasion through the matrigel in a concentration-dependent manner. Exploration of the underlying mechanism demonstrated that RT attenuated the phosphorylation of STAT3 and down-regulated the expression of Nrf2. The above findings suggest a model of RT in suppressing B16F10 cancer cell migration and invasion. It may serve as a promising drug for the treatment of cancer metastasis.

2. Results

2.1. RT Had No Effect on Inflammation-Induced B16F10 Cell Proliferation

Renieramycin T (RT), a bistetrahydroisoquinolinequinone that is extracted from the Thai blue sponge *Xestospongia* sp., in this study, was self-synthesized by our cooperative group. The structure of RT is shown in Figure 1A.

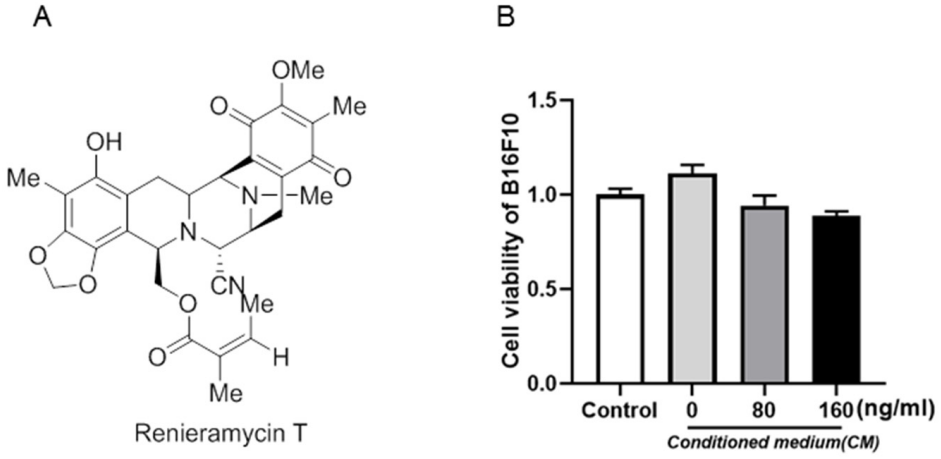

Figure 1. The structure and proliferation effects of renieramycin T (RT) were shown. (**A**) The structure of renieramycin T (RT) is shown. (**B**) RT had no effect on cell proliferation of B16F10 cells in the microenvironment.

To investigate the role of RT in B16F10 cell proliferation, we treated B16F10 cells with various concentrations of RT, the activity of RT against B16F10 cells in a microenvironment was detected by CCK8 method. As shown in Figure 1B, after the control and conditioned cells were treated with RT, the viability of B16F10 cells induced by the supernatant of RAW264.7 was not changed by two concentrations of RT (80 ng/mL and 160 ng/mL). The results indicate that 0–160 ng/mL RT had no significant effect on inflammation-induced B16F10 cell proliferation.

2.2. RT Inhibits the Supernatant of RAW264.7 Cells-Induced B16F10 Cell Migration and Invasion

To explore the function of RT on B16F10 cell migration and invasion, we performed the wound healing assay and Transwell assay. Firstly, the migration ability of B16F10 was detected by scratch test. Compared with the control group, we found that the migration ability of B16F10 induced by RAW264.7 supernatant was enhanced, while the migration ability of B16F10 was reduced after the addition of RT treatment (Figure 2A,B). Correspondingly, the transwell results show that RT reversed the promoting effect of RAW264.7 supernatant on B16F10 invasion (Figure 2C,D). Collectively, these results indicate that RT inhibited the migration and invasion of B16F10 in an inflammatory microenvironment.

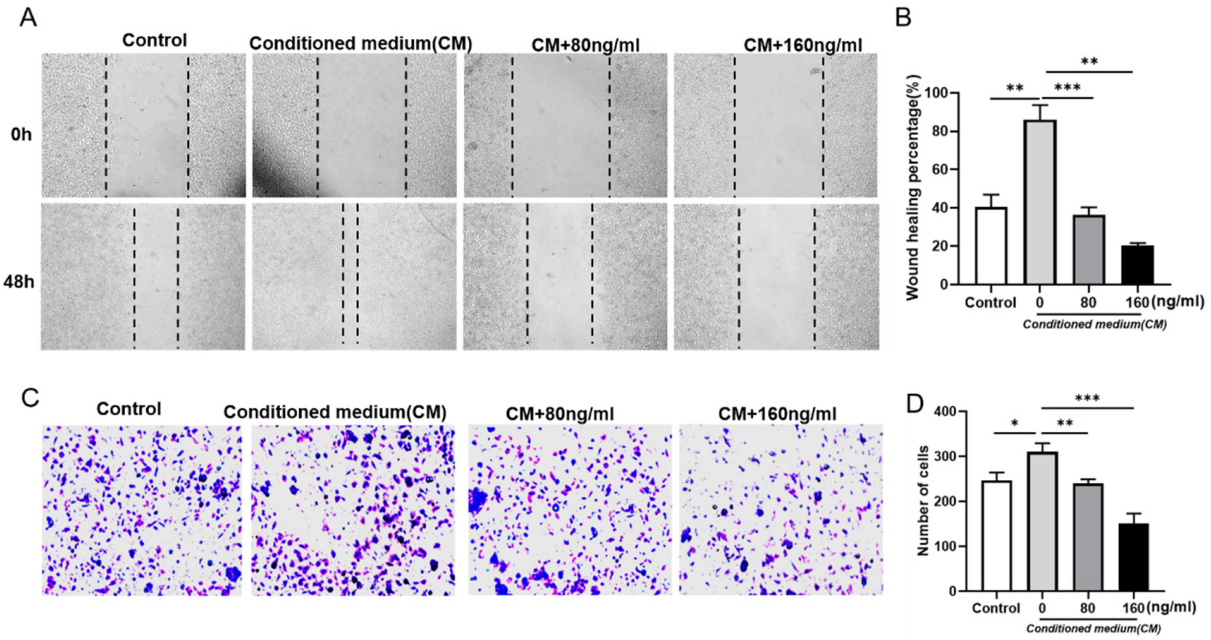

Figure 2. Effect of RT on B16F10 migration in tumor microenvironment. (**A**) Images of cell migration in each group within 48 h of scratch in wound healing experiment; (**B**) Statistics of wound healing area of B16F10 cells (** $p < 0.01$, *** $p < 0.001$). (**C**) Images of groups of cells passing through pores in the Transwell experiment; (**D**) Statistics on the number of B16F10 invaded cells (* $p < 0.05$, ** $p < 0.01$, *** $p < 0.001$).

2.3. RT Inhibited the Expression of Metastasis-Related Genes in RAW264.7 Cells Supernatant-Induced Tumor Cells

To further verify the effect of RT on B16F10 metastasis, we detected the expression of tumor metastasis-related genes twist, snail, vimentin, and N-cadherin by qPCR. We found that RAW264.7 supernatant can enhance the expression of twist, snail, vimentin, and N-cadherin at the transcriptional level compared with the control group, but their expression decreased after RT treatment (Figure 3A–F). Moreover, the Western blotting results also show RAW264.7 supernatant increased the expression of twist, snail, vimentin, and N-cadherin, RT treatment reduced their expression (Figure 3G). The above results further indicate that RT inhibited the metastasis of B16F10 in an inflammatory microenvironment.

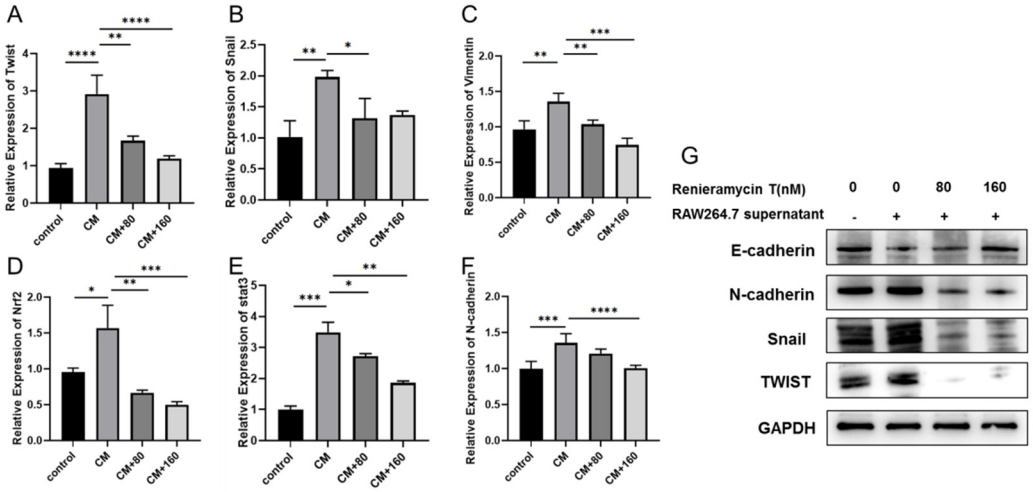

Figure 3. RT inhibits the expression of B16F10 tumor metastasis-related genes. (**A**–**F**) Quantitative analyses of twist, snail, vimentin, and N-cadherin mRNA in B16F10 treated with RT for 48 h at the control and conditioned cells. (**G**) Western blotting was performed to check the expression of twist, snail, vimentin, and N-cadherin in B16F10 treated with RT for 48 h at the control and conditioned cells. (n = 3, * $p < 0.05$, ** $p < 0.01$, *** $p < 0.001$, **** $p < 0.0001$).

2.4. RT Suppressed the STAT3 and Nrf2 Signaling Pathways in B16F10 Cells

In order to explore the mechanism of RT against tumor invasion and metastasis, we detected the effects of RT on the expressions of STAT3, p-STAT3, and Nrf2 in B16F10 cells by Western blots and qPCR. The results show that RAW264.7 supernatant promotes the expression of STAT3, p-STAT3, and Nrf2 protein levels, and the expressions of STAT3, p-STAT3, and Nrf2 were recovered by RT treatment (Figure 4A–D). Similarly, at the mRNA level, RT was found to inhibit the attenuated phosphorylation of STAT3 and down-regulate the expression of Nrf2 induced by supernatant of RAW264.7 (Figure 4E,F). In conclusion, the above results display that RT may inhibit the migration and invasion of B16F10 in an inflammatory microenvironment through Nrf2 and STAT3 signaling pathways.

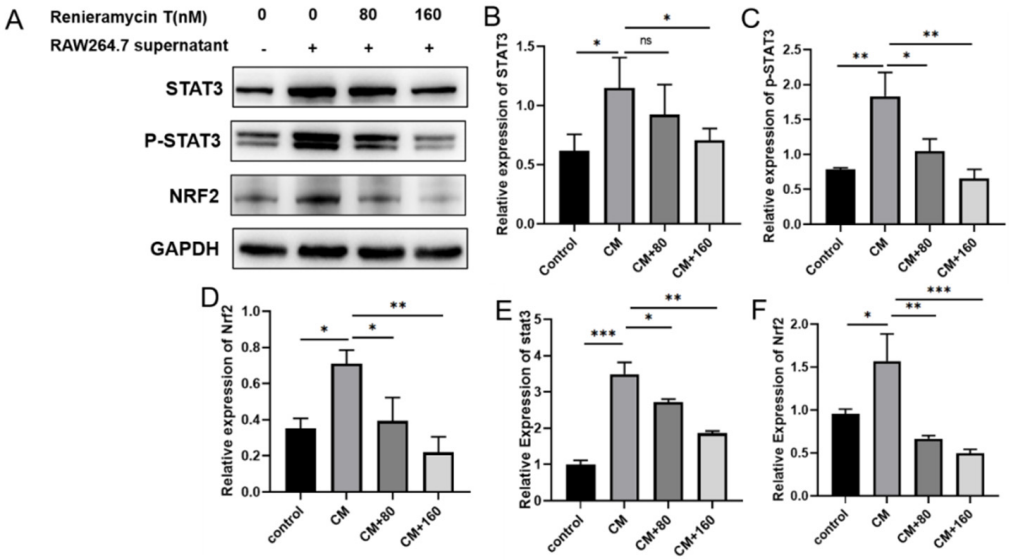

Figure 4. RT repressed the phosphorylation of STAT3 and down-regulated the expression Nrf2 in B16F10 cells. (**A**) The expression of STAT3, p-STAT3, and Nrf2 proteins were detected by WB assay; (**B**–**D**) The relative expression level of p-STAT3, STAT3, and Nrf2 proteins were analyzed in the B16F10 (* $p < 0.05$, ** $p < 0.01$); (**E**,**F**) The relative expression of STAT3 and Nrf2 were detected by qRT-PCR (* $p < 0.05$, ** $p < 0.01$, *** $p < 0.001$).

2.5. Proposed Model of RT in Suppressing B16F10 Cell Migration and Invasion

Based on the totality of our findings, we propose the following model (Figure 5). RT inhibits the migration and invasion of B16F10 treated with RAW264.7 supernatant through Nrf2 and STAT3 signaling pathways.

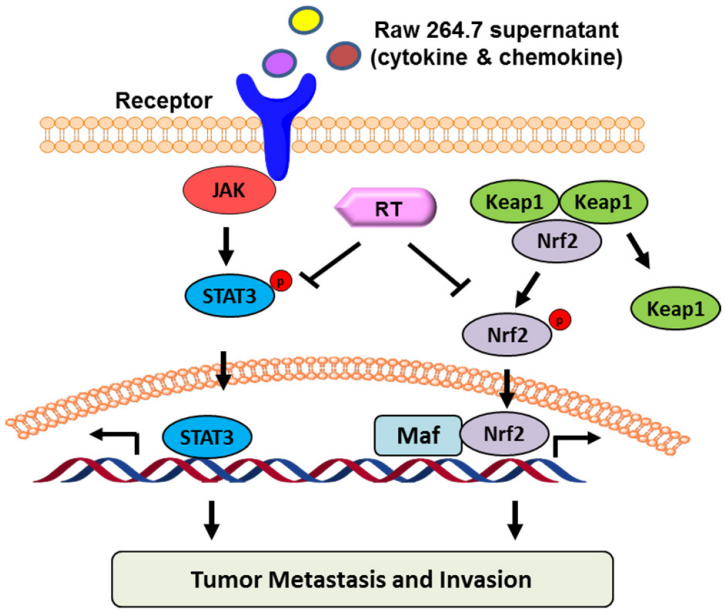

Figure 5. Proposed model of RT suppresses B16F10 cell migration and invasion.

3. Discussion

As one of the major common human malignancies, melanoma has higher morbidity and mortality. As a result of tumor metastasis, clinical success in the surgical treatment of melanoma patients is limited. With the precision medicine developed, it is an urgent need to explore novel, new molecular agents for melanoma metastasis treatment.

Marine tetrahydroisoquinoline alkaloids are one kind of natural products that have a wide range of bioactivities, including anti-tumor, anti-bacteria, anti-virus, anti-inflammation activities, etc [30]. The most famous drug, Ecteinascidin-743 (ET-743), is the first marine antitumor drug to treat soft tissue sarcoma (STS) approved by the European Union in October 2007 [31]. Other small molecules of marine tetrahydroisoquinoline alkaloids, such as reieramycin M, were reported to kill the breast cancer cell MCF-7 by combining with doxorubicin to sensitize Anoikis' resistance of lung cancer cell H460. As one of the marine tetrahydroisoquinoline alkaloids, RT plays a vital role in inhibiting tumor metastasis and invasion. In this study, the anti-metastasis ability of RT was discovered, and the mechanism of RT suppressing melanoma cell migration and invasion was reported for the first time.

Nuclear factor (erythroid-derived 2)-like 2 (Nrf2) is a redox-sensitive transcription factor that plays a key role in cellular cytoprotection against oxidative and electrophilic stress [37,38]. Although Nrf2 protects normal cells against chemically induced tumor formation, it confers an advantage for the survival and growth of many different types of cancer cells [39]. Another transcription factor, STAT3, functions as an oncogene. Persistently activated STAT3 is associated with the proliferation, survival, and invasiveness of tumor cells, including those of breast, lung, pancreatic, and head and neck origin. Recent studies suggested the possibility of the interplay or cross talk between Nrf2 and STAT3 [40,41]. In our studies, RT restrained the phosphorylation of STAT3 and decreased Nrf2 in protein levels, suggesting that the STAT3/Nrf-2 signaling axis might be involved in the mechanism of RT repressing migration and invasion. It is suggested that STAT3/Nrf2 can be an effective target for cancer prevention or treatment. However, the potential manner in which RT inhibits STAT3 and Nrf2 was not clear, and needs to be further studied.

4. Materials and Methods

4.1. Reagent and Antibody

RT was dissolved in dimethyl sulfoxide (DMSO) as a stock solution and stored at −20 °C until needed. The final concentration of DMSO did not exceed 0.1% throughout the study (this concentration was found to have no effect on cell invasion or cell growth). The chemical structure of RT is shown in Figure 1. The compound was prepared at concentrations of 80 ng/mL and 160 ng/mL. Primary antibodies for vimentin (CST, Boston, MA, USA), STAT3 (CST, Boston, MA, USA), p-STAT3 (CST, Boston, MA, USA) and Nrf2 (CST, Boston, MA, USA) were detected by Western blot. Antibody to GAPDH was from Santa Cruz Biotechnology (Santa Cruz, CA, USA). Cell Counting Kit-8 (CCK-8) was purchased from Good Laboratory Practice Bioscience (Glpbio, Montclair, CA, USA). IRDye TM800 conjugated second antibody was obtained from Rockland (Gilbertsville, PA, USA). BCA Protein Assay kit was purchased from Beyotime (Beyotime, Shanghai, China).

4.2. Cell Culture

The mouse melanoma cells B16F10 and the mononuclear cells RAW264.7 were originally obtained from the Cell Bank of Shanghai Institute of Cell Biology. B16F10 cells were cultured in DMEM medium (Gibco, Grand Island, NY, USA) containing 10% fetal bovine serum (Gibco, Grand Island, NY, USA), 100 U/mL penicillin, and 100 mg/L streptomycin. RAW264.7 cells were cultured in RPMI-1640 medium (Gibco, Grand Island, NY, USA) containing 10% heat-inactivated fetal bovine serum, 100 U/mL penicillin, and 100 mg/L streptomycin. Cells were grown in a stable environment with 5% CO_2 at 37 °C.

4.3. Cell Viability Assay

B16F10 cells were plated at a density of 104 cells per well into 96-well plates. After overnight growth, cells were exposed to different concentrations of RT for 48 h in a 5% CO_2 incubator at 37 °C. At the end of treatment, 10 µL of 0.5% CCK-8 was added to the medium and incubated for 4 h at 37 °C. The supernatant was removed and 0.1 mL DMSO was used to dissolve precipitate. Absorbance was measured spectrophotometrically at 450 nm.

4.4. Wound Healing Assay

B16F10 cells were seeded in a six-well plate and allowed to attach overnight to 80% confluency. Subsequently, cell monolayers were wounded by pipette tips and washed with PBS twice to remove floating cells. Cells were treated with or without different concentrations of RT for up to 48 h. Cells migrated into the wound surface and the number of migrating cells was determined under an inverted microscopy at various times; five randomly chosen fields were analyzed for each well. The percentage of inhibition was expressed using untreated wells at 100%. Three independent experiments were performed.

4.5. Transwell Assay

The ability of invasion was demonstrated by transwell assay. The melanoma B16F10 cells were treated with RAW264.7 supernate and different concentrations of RT solutions about 30 min in advance, and they were inoculated at a density of 1.5 × 104 cells in the upper chamber (Thermo Scientific, Shanghai, China), and the chemokine was in the lower chamber. The upper and lower chambers were separated by a polycarbonate membrane and a side near the upper chamber that was carpeted with Matrigel (Becton, Dickinson and Company, San Jose, CA, USA). Eventually, count the quantity of tumor cells.

4.6. Quantitative Real Time-PCR (qRT-PCR)

Total RNA was isolated from the cells using the Trizol reagent (Life Technology, Shanghai, China), and mRNA was reverse-transcribed to cDNA using the GoScript Reverse Transcription System (Vazyme, Nanjing, China). The qRT-PCR was performed in the Applied Biosystems 7500 cycler using the GoTaq qPCR Master Mix (Vazyme, Nanjing, China). The PCR conditions were as follows: pre-denaturation at 95 °C for 30 s, followed by

40 cycles of 95 °C for 10 s, and annealing and extension at 60 °C for 30 s. The relative cDNA levels of FR were calculated by the comparative Ct method, and normalized to GAPDH as the endogenous control (Table 1).

Table 1. Real-time RT-PCR oligonucleotide primer.

Genes	Primer	Sequence (5′-3′)
GAPDH	Forward	GCACCGTCAAGGCTGAGAAC
	Reverse	TGGTGAAGACGCCAGTGGA
Twist	Forward	GTCCGCAGTCTTACGAGGAG
	Reverse	GCTTGAGGGTCTGAATCTTGCT
Snail	Forward	TCGGAAGCCTAACTACAGCGA
	Reverse	AGATGAGCATTGGCAGCGAG
Vimentin	Forward	GACGCCATCAACACCGAGTT
	Reverse	CTTTGTCGTTGGTTAGCTGGT
N-cadherin	Forward	TCAGGCGTCTGTAGAGGCTT
	Reverse	ATGCACATCCTTCGATAAGACTG
STAT3	Forward	CAGCAGCTTGACACACGGTA
	Reverse	AAACACCAAAGTGGCATGTGA
Nrf2	Forward	TCAGCGACGGAAAGAGTATGA
	Reverse	CCACTGGTTTCTGACTGGATGT

4.7. Western Blot

Cells were treated with RAW264.7 supernate and various concentrations of RT for 24 h. Cells were lysed with RIPA buffer, and the mixed protein was separated by SDS-PAGE according to the size of molecule, and transferred to the NC membrane. The membranes were combined with primary antibody to GAPDH, STAT3, p-STAT3, and Nrf2, respectively. They were co-incubated in the room temperature for 2 h. After washing with TBST three times, the membranes were combined by secondary antibody for 1 h at room temperature. The blots were detected with enhanced chemiluminescence (Pierce Chemical, 34080, Rockford, IL, USA) and then analyzed by ImageJ software (National Institutes of Health, Bethesda, MD, USA).

4.8. Statistical Analysis

All the data in our results are shown as means ± standard deviation (SD) from triplicate experiments. Statistically significant differences [analysis of variance (ANOVA) and post hoc tests] were analyzed using the GraphPad Prism software (GraphPad Software Inc., Avenida, CA, USA). Details of each statistical analysis used are provided in the figure legends.

5. Conclusions

In conclusion, we established an inflammation-related tumor model by using the supernatant of RAW264.7 cells to simulate B16F10 mouse melanoma cells. We showed that RT suppressed RAW264.7 cell supernatant-reduced B16F10 cell adhesion to fibronectin-coated substrate, migration, and invasion through the matrigel in a concentration-dependent manner. We explored the underlying mechanism and demonstrated that RT attenuated the phosphorylation of STAT3 and down-regulated the expression of Nrf2. The above findings suggest a model of RT for suppressing B16F10 cancer cell migration and invasion. It may serve as a promising drug for the treatment of cancer metastasis.

Author Contributions: B.Y., X.C., J.Y. and R.C. conceived and designed the experiments; B.Y., J.L., X.L. and R.C. performed the experiments; X.L., J.Y., L.L. and R.C. analyzed the data; X.C. and R.C. wrote the original draft; B.Y. and R.C. obtained funding, reviewed, and edited the draft. All authors have read and agreed to the published version of the manuscript.

Funding: This work was supported by Shandong Medical and Health Science and Technology Development Project (202006020902), and the Key Research and Development Project of Jining (2020YXNS004).

Institutional Review Board Statement: Not applicable.

Informed Consent Statement: Not applicable.

Data Availability Statement: Data are available from the authors upon request.

Conflicts of Interest: The authors declare no conflict of interest.

References

1. Liu, Y.; Li, H.; Liu, F.; Gao, L.B.; Han, R.; Chen, C.; Ding, X.; Li, S.; Lu, K.; Yang, L.; et al. Heterogeneous nuclear ribonucleoprotein A2/B1 is a negative regulator of human breast cancer metastasis by maintaining the balance of multiple genes and pathways. *EBioMedicine* **2020**, *51*, 102583. [CrossRef] [PubMed]
2. Denecker, G.; Vandamme, N.; Akay, O.; Koludrovic, D.; Taminau, J.; Lemeire, K.; Gheldof, A.; De Craene, B.; Van Gele, M.; Brochez, L.; et al. Identification of a ZEB2-MITF-ZEB1 transcriptional network that controls melanogenesis and melanoma progression. *Cell Death Differ.* **2014**, *21*, 1250–1261. [CrossRef] [PubMed]
3. Dang, N.N.; Jiao, J.; Meng, X.; An, Y.; Han, C.; Huang, S. Abnormal overexpression of G9a in melanoma cells promotes cancer progression via upregulation of the Notch1 signaling pathway. *Aging (Albany N. Y.)* **2020**, *12*, 2393–2407. [CrossRef] [PubMed]
4. Han, Y.H.; Mun, J.G.; Jeon, H.D.; Park, J.; Kee, J.Y.; Hong, S.H. Gomisin A ameliorates metastatic melanoma by inhibiting AMPK and ERK/JNK-mediated cell survival and metastatic phenotypes. *Phytomedicine* **2020**, *68*, 153147. [CrossRef] [PubMed]
5. Javelaud, D.; Mohammad, K.S.; McKenna, C.R.; Fournier, P.; Luciani, F.; Niewolna, M.; André, J.; Delmas, V.; Larue, L.; Guise, T.A.; et al. Stable overexpression of Smad7 in human melanoma cells impairs bone metastasis. *Cancer Res.* **2007**, *67*, 2317–2324. [CrossRef] [PubMed]
6. Wu, Z.; Liu, W.; Wang, Z.; Zeng, B.; Peng, G.; Niu, H.; Chen, L.; Liu, C.; Hu, Q.; Zhang, Y.; et al. Mesenchymal stem cells derived from iPSCs expressing interleukin-24 inhibit the growth of melanoma in the tumor-bearing mouse model. *Cancer Cell Int.* **2020**, *20*, 33. [CrossRef]
7. Robinson, B.D.; Jones, J.G. Tumor microenvironment of metastasis (TMEM): A novel tissue-based assay for metastatic risk in breast cancer. *Future Oncol.* **2009**, *5*, 919–921. [CrossRef]
8. Mantovani, A.; Sica, A. Macrophages, innate immunity and cancer: Balance, tolerance, and diversity. *Curr. Opin. Immunol.* **2010**, *22*, 231–237. [CrossRef]
9. Kuo, C.; Yang, T.; Tsai, P.; Yu, C. Role of the Inflammatory Response of RAW 264.7 Cells in the Metastasis of Novel Cancer Stem-Like Cells. *Medicina (Kaunas)* **2021**, *57*, 778. [CrossRef]
10. Wang, Q.; Ni, H.; Lan, L.; Wei, X.; Xiang, R.; Wang, Y. Fra-1 protooncogene regulates IL-6 expression in macrophages and promotes the generation of M2d macrophages. *Cell Res.* **2010**, *20*, 701–712. [CrossRef]
11. Yang, J.; Zhang, Z.; Chen, C.; Liu, Y.; Si, Q.; Chuang, T.H.; Li, N.; Gomez-Cabrero, A.; Reisfeld, R.A.; Xiang, R.; et al. MicroRNA-19a-3p inhibits breast cancer progression and metastasis by inducing macrophage polarization through downregulated expression of Fra-1 proto-oncogene. *Oncogene* **2014**, *33*, 3014–3023. [CrossRef]
12. Abdel-Gaber, S.A.; Geddawy, A.; Moussa, R.A. The hepatoprotective effect of sitagliptin against hepatic ischemia reperfusion-induced injury in rats involves Nrf-2/HO-1 pathway. *Pharmacol. Rep.* **2019**, *71*, 1044–1049. [CrossRef] [PubMed]
13. Zuo, J.; Zhao, M.; Fan, Z.; Liu, B.; Wang, Y.; Li, Y.; Lv, P.; Xing, L.; Zhang, X.; Shen, H. MicroRNA-153-3p regulates cell proliferation and cisplatin resistance via Nrf-2 in esophageal squamous cell carcinoma. *Thorac. Cancer* **2020**, *11*, 738–747. [CrossRef] [PubMed]
14. Lu, Y.; Hu, P.; Zhou, H.; Yang, Z.; Sun, Y.; Hoffman, R.M.; Chen, J. Double-negative T Cells Inhibit Proliferation and Invasion of Human Pancreatic Cancer Cells in Co-culture. *Anticancer Res.* **2019**, *39*, 5911–5918. [CrossRef] [PubMed]
15. Kim, Y.R.; Oh, J.E.; Kim, M.S.; Kang, M.R.; Park, S.W.; Han, J.Y.; Eom, H.S.; Yoo, N.J.; Lee, S.H. Oncogenic NRF2 mutations in squamous cell carcinomas of oesophagus and skin. *J. Pathol.* **2010**, *220*, 446–451. [CrossRef]
16. Kitamura, H.; Onodera, Y.; Murakami, S.; Suzuki, T.; Motohashi, H. IL-11 contribution to tumorigenesis in an NRF2 addiction cancer model. *Oncogene* **2017**, *36*, 6315–6324. [CrossRef]
17. Rachakonda, G.; Sekhar, K.R.; Jowhar, D.; Samson, P.C.; Wikswo, J.P.; Beauchamp, R.D.; Datta, P.K.; Freeman, M.L. Increased cell migration and plasticity in Nrf2-deficient cancer cell lines. *Oncogene* **2010**, *29*, 3703–3714. [CrossRef]
18. Lignitto, L.; LeBoeuf, S.E.; Homer, H.; Jiang, S.; Askenazi, M.; Karakousi, T.R.; Pass, H.I.; Bhutkar, A.J.; Tsirigos, A.; Ueberheide, B.; et al. Nrf2 Activation Promotes Lung Cancer Metastasis by Inhibiting the Degradation of Bach1. *Cell* **2019**, *178*, 316–329.e18. [CrossRef]
19. Huang, S. Regulation of metastases by signal transducer and activator of transcription 3 signaling pathway: Clinical implications. *Clin. Cancer Res.* **2007**, *13*, 1362–1366. [CrossRef]
20. Nam, S.; Buettner, R.; Turkson, J.; Kim, D.; Cheng, J.; Muehlbeyer, S.; Hippe, F.; Vatter, S.; Merz, K.H.; Eisenbrand, G.; et al. Indirubin derivatives inhibit Stat3 signaling and induce apoptosis in human cancer cells. *Proc. Natl. Acad. Sci. USA* **2005**, *102*, 5998–6003. [CrossRef]

21. Kang, T.; Wang, W.; Zhong, H.; Dong, Z.; Huang, Q.; Mok, S.; Leung, C.; Wong, V.; Ma, D. An anti-prostate cancer benzofuran-conjugated iridium(III) complex as a dual inhibitor of STAT3 and NF-κB. *Cancer Lett.* **2017**, *396*, 76–84. [CrossRef] [PubMed]
22. Onimoe, G.; Liu, A.; Lin, L.; Wei, C.; Schwartz, E.; Bhasin, D.; Li, C.; Fuchs, J.; Li, P.; Houghton, P.; et al. Small molecules, LLL12 and FLLL32, inhibit STAT3 and exhibit potent growth suppressive activity in osteosarcoma cells and tumor growth in mice. *Investig. New Drugs* **2012**, *30*, 916–926. [CrossRef] [PubMed]
23. Ma, D.; Liu, L.; Leung, K.; Chen, Y.; Zhong, H.; Chan, D.; Wang, H.; Leung, C. Antagonizing STAT3 dimerization with a rhodium(III) complex. *Angew. Chem. Int. Ed.* **2014**, *53*, 9178–9182. [CrossRef] [PubMed]
24. Niu, G.; Heller, R.; Catlett-Falcone, R.; Coppola, D.; Jaroszeski, M.; Dalton, W.; Jove, R.; Yu, H. Gene therapy with dominant-negative Stat3 suppresses growth of the murine melanoma B16 tumor in vivo. *Cancer Res.* **1999**, *59*, 5059–5063. [PubMed]
25. Zhang, X.; Zhang, Y.; He, Z.; Yin, K.; Li, B.; Zhang, L.; Xu, Z. Chronic stress promotes gastric cancer progression and metastasis: An essential role for ADRB2. *Cell Death Dis.* **2019**, *10*, 788. [CrossRef] [PubMed]
26. Zheng, M.; Cao, M.; Luo, X.; Li, L.; Wang, K.; Wang, S.; Wang, H.; Tang, Y.; Tang, Y.; Liang, X. EZH2 promotes invasion and tumour glycolysis by regulating STAT3 and FoxO1 signalling in human OSCC cells. *J. Cell Mol. Med.* **2019**, *23*, 6942–6954. [CrossRef] [PubMed]
27. Liu, Z.; Wang, H.; Guan, L.; Lai, C.; Yu, W.; Lai, M. LL1, a novel and highly selective STAT3 inhibitor, displays anti-colorectal cancer activities in vitro and in vivo. *Br. J. Pharmacol.* **2020**, *177*, 298–313. [CrossRef]
28. Wang, F.; Ma, X.; Mao, G.; Zhang, X.; Kong, Z. STAT3 enhances radiation-induced tumor migration, invasion and stem-like properties of bladder cancer. *Mol. Med. Rep.* **2021**, *23*, 87. [CrossRef]
29. Liang, J.; Nagahashi, M.; Kim, E.Y.; Harikumar, K.B.; Yamada, A.; Huang, W.C.; Hait, N.C.; Allegood, J.C.; Price, M.M.; Avni, D.; et al. Sphingosine-1-phosphate links persistent STAT3 activation, chronic intestinal inflammation, and development of colitis-associated cancer. *Cancer Cell* **2013**, *23*, 107–120. [CrossRef]
30. Scott, J.D.; Williams, R.M. Chemistry and biology of the tetrahydroisoquinoline antitumor antibiotics. *Chem. Rev.* **2002**, *102*, 1669–1730. [CrossRef]
31. Cuevas, C.; Francesch, A. Development of Yondelis (trabectedin, ET-743). A semisynthetic process solves the supply problem. *Nat. Prod. Rep.* **2009**, *26*, 322–337. [CrossRef] [PubMed]
32. Jia, J.; Chen, R.; Liu, H.; Li, X.; Jia, Y.; Chen, X. Asymmetric synthesis of (-)-renieramycin T. *Org. Biomol. Chem.* **2016**, *14*, 7334–7344. [CrossRef] [PubMed]
33. Petsri, K.; Chamni, S.; Suwanborirux, K.; Saito, N.; Chanvorachote, P. Renieramycin T Induces Lung Cancer Cell Apoptosis by Targeting Mcl-1 Degradation: A New Insight in the Mechanism of Action. *Mar. Drugs* **2019**, *17*, 301. [CrossRef] [PubMed]
34. Chantarawong, W.; Chamni, S.; Suwanborirux, K.; Saito, N.; Chanvorachote, P. 5-O-Acetyl-Renieramycin T from Blue Sponge Xestospongia sp. Induces Lung Cancer Stem Cell Apoptosis. *Mar. Drugs* **2019**, *17*, 109. [CrossRef] [PubMed]
35. Petsri, K.; Yokoya, M.; Tungsukruthai, S.; Rungrotmongkol, T.; Nutho, B.; Vinayanuwattikun, C.; Saito, N.; Takehiro, M.; Sato, R.; Chanvorachote, P. Structure-Activity Relationships and Molecular Docking Analysis of Mcl-1 Targeting Renieramycin T Analogues in Patient-derived Lung Cancer Cells. *Cancers* **2020**, *12*, 875. [CrossRef]
36. Suksamai, D.; Racha, S.; Sriratanasak, N.; Chaotham, C.; Aphicho, K.; Lin, A.C.K.; Chansriniyom, C.; Suwanborirux, K.; Chamni, S.; Chanvorachote, P. 5-O-(N-Boc-l-Alanine)-Renieramycin T Induces Cancer Stem Cell Apoptosis via Targeting Akt Signaling. *Mar. Drugs* **2022**, *20*, 235. [CrossRef]
37. Mallard, A.R.; Spathis, J.G.; Coombes, J.S. Nuclear factor (erythroid-derived 2)-like 2 (Nrf2) and exercise. *Free. Radic. Biol. Med.* **2020**, *160*, 471–479. [CrossRef]
38. Ferrándiz, M.L.; Nacher-Juan, J.; Alcaraz, M.J. Nrf2 as a therapeutic target for rheumatic diseases. *Biochem. Pharm.* **2018**, *152*, 338–346. [CrossRef]
39. Kim, S.J.; Saeidi, S.; Cho, N.C.; Kim, S.H.; Lee, H.B.; Han, W.; Noh, D.Y.; Surh, Y.J. Interaction of Nrf2 with dimeric STAT3 induces IL-23 expression: Implications for breast cancer progression. *Cancer Lett.* **2021**, *500*, 147–160. [CrossRef]
40. Hou, T.; Yang, M.; Yan, K.; Fan, X.; Ci, X.; Peng, L. Amentoflavone Ameliorates Carrageenan-Induced Pleurisy and Lung Injury by Inhibiting the NF-κB/STAT3 Pathways via Nrf2 Activation. *Front. Pharmacol.* **2022**, *13*, 763608. [CrossRef]
41. Li, C.; Wang, R.; Zhang, Y.; Hu, C.; Ma, Q. PIAS3 suppresses damage in an Alzheimer's disease cell model by inducing the STAT3-associated STAT3/Nestin/Nrf2/HO-1 pathway. *Mol. Med.* **2021**, *27*, 150. [CrossRef] [PubMed]